Reply to comments

Journal: Atmospheric Chemistry and Physics

Manuscript Number: acp-2022-440

Title: "High frequency of new particle formation events driven by summer monsoon in the central Tibetan Plateau, China"

Author(s): Lizi Tang, Min Hu, Dongjie Shang, Xin Fang, Jianjiong Mao, Wanyun Xu, Jiacheng Zhou, Weixiong Zhao, Yaru Wang, Chong Zhang, Yingjie Zhang, Jianlin Hu, Limin Zeng, Chunxiang Ye, Song Guo, Zhijun Wu

I. Reply to Reviewer 2

Reply to Reviewer 2's overall comments:

New particle formation (NPF) at high altitudes is crucial to understand sources of aerosol and CCN in the free troposphere. In this study, the authors conducted intensive measurements at Nam Co station (4379 m a.s.l) in the central TP to understand the new particle formation during pre-monsoon and monsoon seasons. They identified the frequency of NPF during monsoon seasons was significantly higher than during pre-monsoon seasons. This study did provide valuable observation data. But the explanation that higher VOCs triggered the frequent NPF during monsoon season is unconvincing. Therefore, the manuscript is not recommended to be published on ACP unless the authors can address the following major concerns.

We appreciate the comments from the reviewer on this manuscript. We have answered them point to point in the following paragraphs (the texts italicized are the comments, the texts indented are the responses, and the texts in blue are revised parts in new manuscript). In addition, all changes made are marked in the revised manuscript.

Reply to Reviewer 2's comments (3):

1. Sulfuric acid (SA), Ultra/Extremely Low Volatility Organic Compounds (U/ELVOCs), and bases, e.g., NH3 or DMA, are known as the essential precursor of NPF. Their concentrations determine whether NPF can occur, as well as the intensity. However, in this study, all these key precursors were not measured. Even the precursors of these "direct precursors", e.g. SO2 and VOCs who can form low-volatile oxidation products, were not well measured either. First, the simulated concentration of SO2 used in this study without any verification by observation data is not convincing. Since SO2 is a very reactive species, one

needs to use the simulated value very carefully. Second, although 99 types of VOCs were measured during pre-monsoon using a GC-MS/FID, they are key precursors of ozone formation and are not suitable as indicator precursors for ELVOCs. The author, at least, needs to provide the concentration of monoterpenes, which are well-known sources of ELVOCs. In addition, the simulation of VOCs during monsoon is needed to be verified. In summary, the authors need to provide more solid evidence to support their main conclusion that higher VOCs triggered the frequent NPF during monsoon season.

Thanks for the comment. The measurements of the NPF precursors including SO_2 and VOC are limited due to the harsh conditions and logistical limitations, with only VOC in pre-monsoon season. So we utilized WRF/CMAQ modeling system to simulate the levels of SO_2 and VOC in the whole observation period, to assist in the analysis of the role of sulfuric acid and organics. As for the verification of the simulated SO_2 and VOC, we have added the analysis on statistical parameters of model evaluation and correlation analysis with other tracers in the revised manuscript. Firstly, the WRF/CMAQ models successfully reproduced the meteorological fields and air pollutants including PM and O_3 with model performance indices meeting the suggested benchmarks, which means the simulated meteorological fields and particulate and gaseous pollutants are qualitied. For VOC, the observed VOC and predicted VOC in pre-monsoon season were compared to examine the model performance. The benchmarks for VOC had not been reported, but the statistical metrics of MFB (mean fractional bias, -0.47) and MFE (mean fractional error, 0.49) in this study are within the range reported in previous VOC modelling result (Hu et al., 2017). The correlation coefficient (R) between simulated and observed VOC is 0.41, which reflected that the model can fairly simulate the variation of VOC concentration. For SO_2, the WRF/CMAQ models have been successfully reproduced SO_2 in major regions in China with R of 0.25-0.79 (Mao et al., 2022). The simulated SO_2 level in the model domain is comparable with that measured at Mt. Yulong (Shang et al., 2018), with average values of 0.03 ± 0.02 ppbv and 0.06 ± 0.05 ppbv. At the same time, considering that both BC and SO_2 are mainly emitted from coal combustion and biomass burning, BC could be a good indicator for SO_2 especially for pristine environment without local anthropogenic source emissions. A good correlation between SO_2 and BC measured at Mt. Yulong was found with correlation coefficient (R) of 0.79 (Shang et al., 2018). In this study, the modelled SO_2 and measured BC also showed good correlation with R of 0.58. In general, the results of model simulation showed good performance in statistical parameters and correlation analysis with other tracers. The modelled VOC and SO_2 could be used for the NPF analysis.

As for monoterpene such as α-pinene, unfortunately, it was not measured in this study. And there can be some other reference compound such as OVOC for understanding new particle formation from tree

emissions as indicated by the plant chamber experiment (Mentel et al., 2009). In addition, recent studies showed that aromatic compounds such as benzene, toluene, and naphthalene, and C6–C10 alkanes can produce considerable amounts of highly oxygenated products through multi-generation OH oxidation or autoxidation (Garmash et al., 2020; Wang et al., 2021), which may trigger the occurrence of NPF events. Therefore, we prefer that different VOC can affect the occurrence of NPF, and we mainly use the concentration of total VOC for analysis.

On the whole, we examined the potential reasons for the distinct NPF frequency using the measured CS, precursors, meteorology and simulated SO_2 and VOC. The comprehensive analysis points to the important role of organics. The higher NPF frequency driven by the higher organics concentration in monsoon season can be supported in one recent research which has found that the concentration of monoterpene-derived HOMs in East Asia was higher in summer (June-August) than that in Spring (March-May) by using GEOS-Chem global chemical transport model (Xu et al., 2022).

Hu, J., Chen, J., Ying, Q., and Zhang, H.: One-year simulation of ozone and particulate matter in China using WRF/CMAQ modeling system, Atmos. Chem. Phys., 16, 10333-10350, 10.5194/acp-16-10333-2016, 2016.

Shang, D., Hu, M., Zheng, J., Qin, Y., Du, Z., Li, M., Fang, J., Peng, J., Wu, Y., Lu, S., and Guo, S.: Particle number size distribution and new particle formation under the influence of biomass burning at a high altitude background site at Mt. Yulong (3410 m), China, Atmos. Chem. Phys., 18, 15687-15703, 10.5194/acp-18-15687-2018, 2018.

Mao, J., Li, L., Li, J., Sulaymon, I. D., Xiong, K., Wang, K., Zhu, J., Chen, G., Ye, F., Zhang, N., Qin, Y., Qin, M., and Hu, J.: Evaluation of Long-Term Modeling Fine Particulate Matter and Ozone in China During 2013–2019, Frontiers in Environmental Science, 10, 10.3389/fenvs.2022.872249, 2022.

Mentel, T. F., Wildt, J., Kiendler-Scharr, A., Kleist, E., Tillmann, R., Dal Maso, M., Fisseha, R., Hohaus, T., Spahn, H., Uerlings, R., Wegener, R., Griffiths, P. T., Dinar, E., Rudich, Y., and Wahner, A.: Photochemical production of aerosols from real plant emissions, Atmos. Chem. Phys., 9, 4387-4406, 10.5194/acp-9-4387-2009, 2009.

Garmash, O., Rissanen, M. P., Pullinen, I., Schmitt, S., Kausiala, O., Tillmann, R., Zhao, D., Percival, C., Bannan, T. J., Priestley, M., Hallquist, Å. M., Kleist, E., Kiendler-Scharr, A., Hallquist, M., Berndt, T., McFiggans, G., Wildt, J., Mentel, T. F., and Ehn, M.: Multi-generation OH oxidation as a source for highly oxygenated organic molecules from aromatics, Atmos. Chem. Phys., 20, 515-537, 10.5194/acp-20-515-2020, 2020.

Wang, Z., Ehn, M., Rissanen, M. P., Garmash, O., Quéléver, L., Xing, L., Monge-Palacios, M., Rantala, P., Donahue, N. M., Berndt, T., and Sarathy, S. M.: Efficient alkane oxidation under combustion engine and atmospheric conditions, Communications Chemistry, 4, 18, 10.1038/s42004-020-00445-3, 2021.

Xu, R., Thornton, J. A., Lee, B. H., Zhang, Y., Jaeglé, L., Lopez-Hilfiker, F. D., Rantala, P., and Petäjä, T.: Global simulations of monoterpene-derived peroxy radical fates and the distributions of highly oxygenated organic molecules (HOMs) and accretion products, Atmos. Chem. Phys., 22, 5477-5494, 10.5194/acp-22-5477-2022, 2022.

“**2.3 Model simulation**

Considering the limited measurements on SO_2 and VOC in this observation (only VOC during pre-monsoon season), Weather Research and Forecasting/Community Multiscale Air Quality (WRF/CMAQ) modeling system was adopted to simulate the level of SO_2 and VOC in the whole observation period, to assist in the analysis of the role of sulfuric acid and organics in NPF events.

Weather Research and Forecasting (WRF) (version 4.2.1) model was used to simulate the meteorological

conditions with the FNL reanalysis dataset. The 6 h FNL data were obtained from the U.S. National Centre for Atmospheric Research (NCAR), with a spatial resolution of 1.0° × 1.0° (http://rda.ucar.edu/datasets/ds083.2/, last accessed on 28 April 2022). The Community Multiscale Air Quality version 5.3.2 (CMAQv5.3.2) model, being one of the three-dimensional chemical transport models (CTMs) (Appel et al., 2021), configured with the gas-phase mechanism of SAPRC07tic and the aerosol module of AERO6i, was employed in this study to simulate the air quality over Tibet in the observation period (26 April to 22 May and 15 June to 25 June in 2019). Air quality simulations were performed with a horizontal resolution of 12 km. The corresponding domain covered Tibet and the surrounding countries and regions with 166 × 166 grids (Fig. S2), with the 18 layers in vertical resolution. Detailed information about the model setting is provided in Text S2.

The Multi-resolution Emission Inventory for China version 1.3 (MEICv1.3) (http://www.meicmodel.org) and Regional Emission inventory in ASia (REASv3.2) (https://www.nies.go.jp/REAS/) were used to provide the anthropogenic emissions from China and neighboring countries and regions, respectively. The MEICv1.3 emissions of the year 2019 were used. For REAS, the emission inventory in the year 2015 was used for 2019 as no emission inventory was released for the years after 2015. Although emission inventories are usually released 3 years behind, we acknowledge that this may cause additional uncertainties in the simulation. Biogenic emissions were generated using the Model for Emissions of Gases and Aerosols from Nature (MEGANv2.1) (Guenther et al., 2012). The open biomass burning emissions were processed using the Fire Inventory for NCAR (FINN) during the entire study period (Wiedinmyer et al., 2011).

The model evaluation is introduced in Text S2. The WRF and CMAQ models successfully reproduced the meteorological fields and air pollutants including PM and O_3 with model performance indices meeting the suggested benchmarks. For VOC, the observed VOC and predicted VOC in pre-monsoon season were compared to examine the model performance. The benchmarks for VOC had not been reported, but the statistical metrics of MFB (mean fractional bias, -0.47) and MFE (mean fractional error, 0.49) in this study are within the range reported in previous VOC modelling result (Hu et al., 2017). The correlation coefficient (R) between simulated and observed VOC is 0.41, which reflected that the model can fairly simulate the variation of VOC concentration. It should be noted that VOC was underpredicted on the whole, which may due to the uncertainty of the emission inventory as mentioned before. For SO_2, the WRF/CMAQ models have been successfully reproduced SO_2 in major regions in China with R of 0.25-0.79 (Mao et al., 2022). The simulated SO_2 level in the model domain is comparable with that measured at Mt. Yulong (Shang et al., 2018), with average values of 0.03±0.02 ppbv and 0.06±0.05 ppbv. At the same time, considering that both BC and SO_2 are mainly emitted from coal combustion and biomass burning, BC could be a good indicator for SO_2 especially for pristine environment without local anthropogenic source emissions. As shown in Fig.S6, a good correlation between SO_2 and BC measured at Mt. Yulong was found with correlation coefficient (R) of 0.79 (Shang et al., 2018). In this study, the modelled SO_2 and measured BC also showed good correlation

with R of 0.58 (Fig. S6). In general, the results of model simulation showed good performance in statistical parameters and correlation analysis with other tracers. The modelled VOC and SO2 may be helpful for the NPF analysis."

"**2.3 Text S2 Model simulation**

Model Configurations

The meteorological conditions were simulated using the Weather Research and Forecasting (WRF) (version 4.2.1) model with the FNL reanalysis dataset. The 6 h FNL data were obtained from the U.S. National Centre for Atmospheric Research (NCAR), with a spatial resolution of 1.0° × 1.0° (http://rda.ucar.edu/datasets/ds083.2/, last accessed on 28 April 2022). The physical parameterizations used in this study are the Thompson microphysical process, RRTMG longwave/shortwave radiation scheme; Noah land-surface scheme; MYJ boundary layer scheme; and modified Tiedtke cumulus parameterization scheme. The detailed configuration settings could be found in the works of Hu et al. (2016), Mao et al. (2022), Wang et al. (2021a).

The Community Multiscale Air Quality version 5.3.2 (CMAQv5.3.2) model, being one of the three-dimensional chemical transport models (CTMs) (Appel et al., 2021), configured with the gas-phase mechanism of SAPRC07tic and the aerosol module of AERO6i, was employed in this study to simulate the air quality over Tibet from 24 April to 24 May and 13 June to 27 June in 2019, which contains the observation period. Air quality simulations were performed with a horizontal resolution of 12 km. The corresponding domain covered Tibet and the surrounding countries and regions with 166 × 166 grids (Fig. S2), with the 18 layers in vertical resolution. The initial and boundary conditions were provided by the default profiles. The simulated results of the first two days were not included in the model analysis, which served as a spin-up and reduced the effects of the initial conditions on the simulated results.

Model Evaluation

Previous studies have investigated the impacts of meteorological conditions on the formation, transportation, and dissipation of air pollutants (Hu et al., 2016; Hua et al., 2021; Mao et al., 2022; Sulaymon et al., 2021b; Sulaymon et al., 2021a). Therefore, the evaluation of the WRF model performance was carried out before the usage of its meteorological fields in the CMAQ simulations. The evaluation of the WRF model was achieved by comparing the predicted wind speed (WS, m/s), wind direction (WD, °) at 10 m above the surface, RH (%) and temperature (T, ℃) to the observed values. Fig. S3 showed that WS was well simulated both in pre-monsoon and monsoon seasons. WD was well simulated in pre-monsoon season, and there seems to be some deviation in the simulation of north wind in monsoon season. The main reason about the deviation in WD may be due to the poor terrain and complicated weather conditions. Nevertheless, both simulations and measurements showed more frequent southerly winds during monsoon season. RH and temperature were well simulated in the whole periods (Fig. S4). The good model performance with the statistical metrics of WS, RH and temperature meeting the

suggested benchmarks are shown in Table S1. Generally, the simulated meteorological fields were qualitied and can be further utilized in driving the CMAQ model

Fig. S5 showed the comparison of simulated hourly mean concentration about PM, O_3 and VOC in observation site, which were simulated by CMAQ. The statistical indices used in evaluating the CMAQ model were present in Table S2. It can be seen that PM and O_3 meet the suggested benchmarks, which reflect the good model performance. The observed VOC and predicted VOC in pre-monsoon season were compared to examine the model performance. The benchmarks for VOC had not been reported, but the MFB (mean fractional bias) and MFE (mean fractional error) values are within the range reported in previous VOC modelling result (Hu et al., 2017). The correlation coefficient (R) between simulated and observed VOC is 0.41, which reflected that the model can fairly simulate the variation of VOC concentration. It should be noted that VOC was underpredicted on the whole, which may due to the uncertainty of the emission inventory.

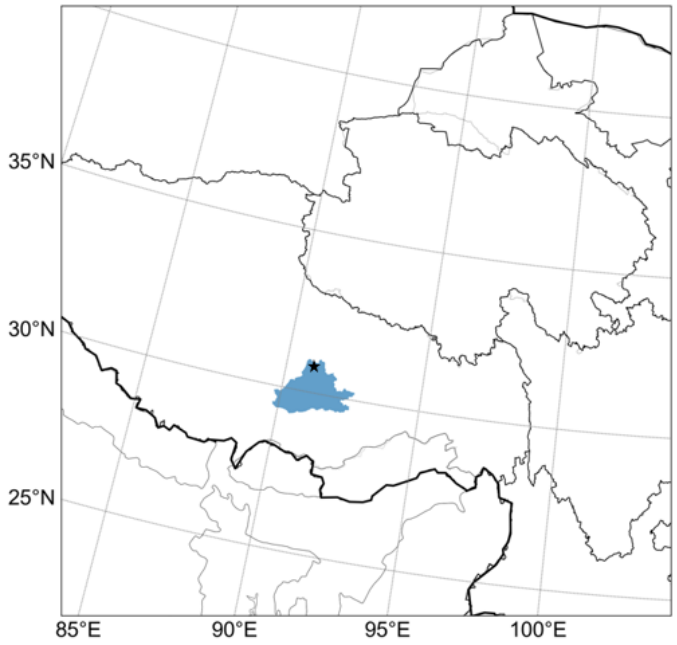

Figure S2. WRF/CMAQ modeling domain

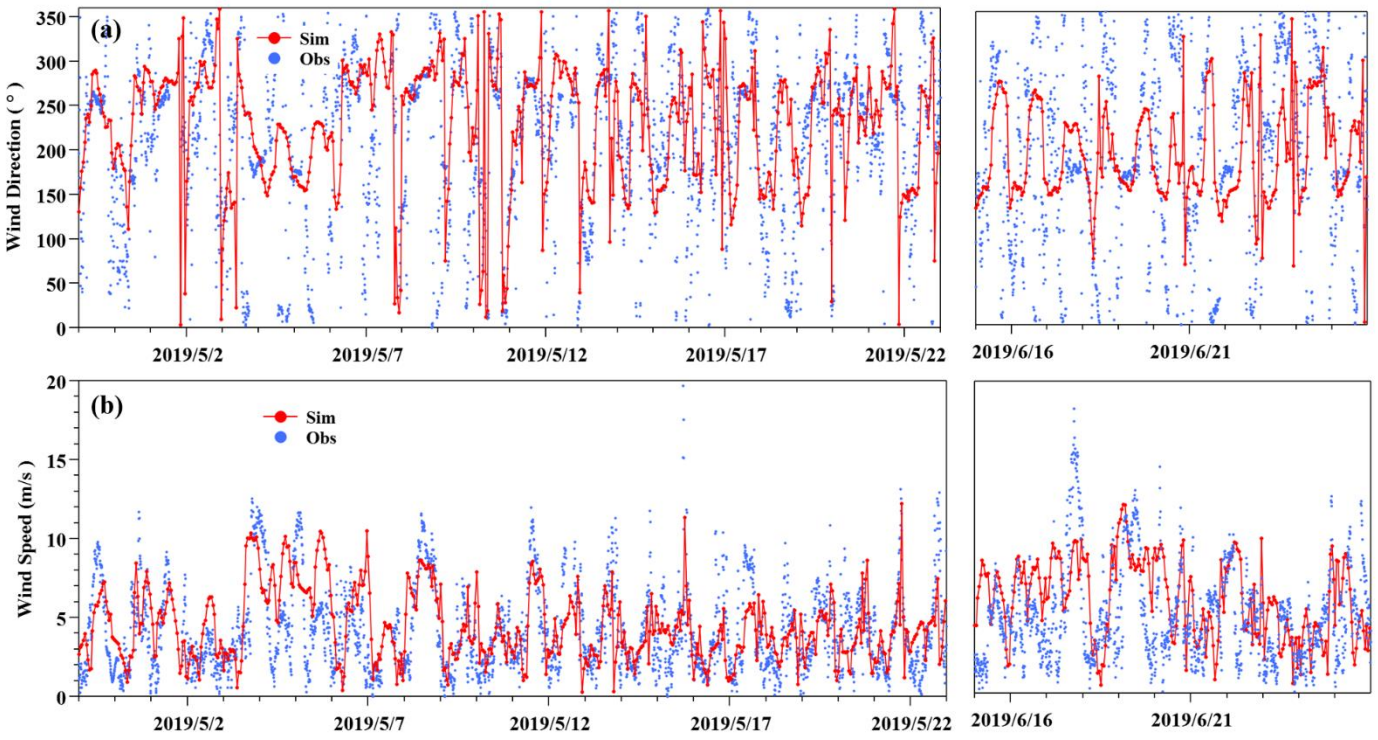

Figure S3. Comparison of simulated (in red dot-line) and observed (in blue dot) wind direction (WD, °) and wind speed (WS, m/s). Observed is 10 minutes mean data. Simulated is hourly mean data.

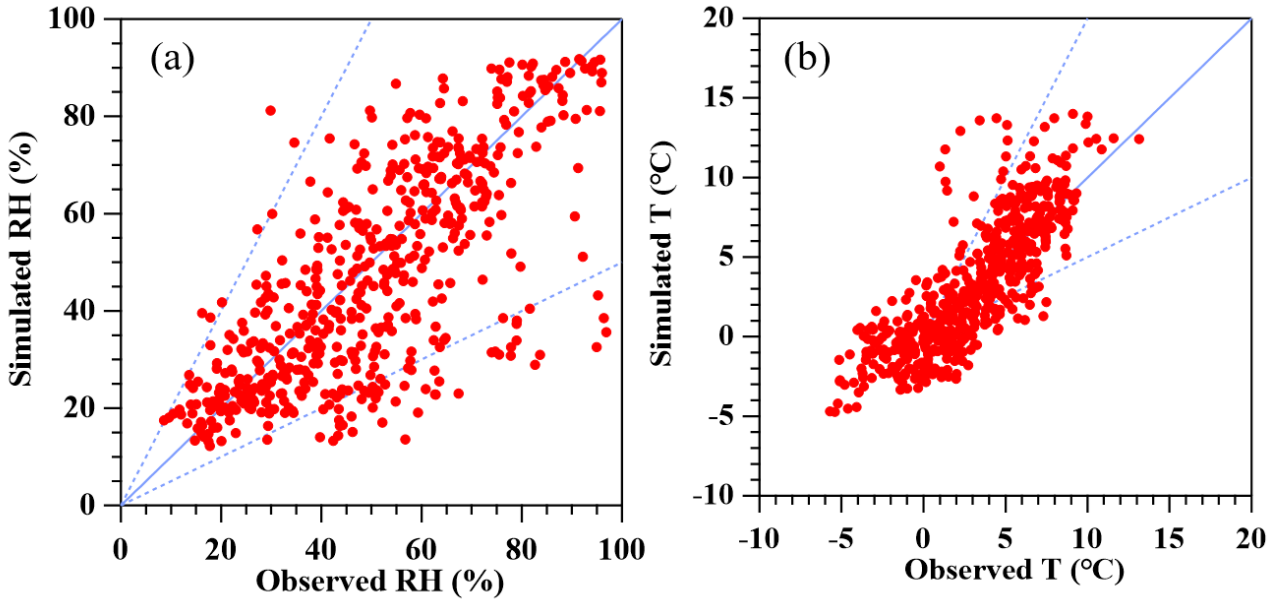

Figure S4. Comparison of simulated and observed RH (%) and temperature (T, °C). RH and temperature are hourly mean data.

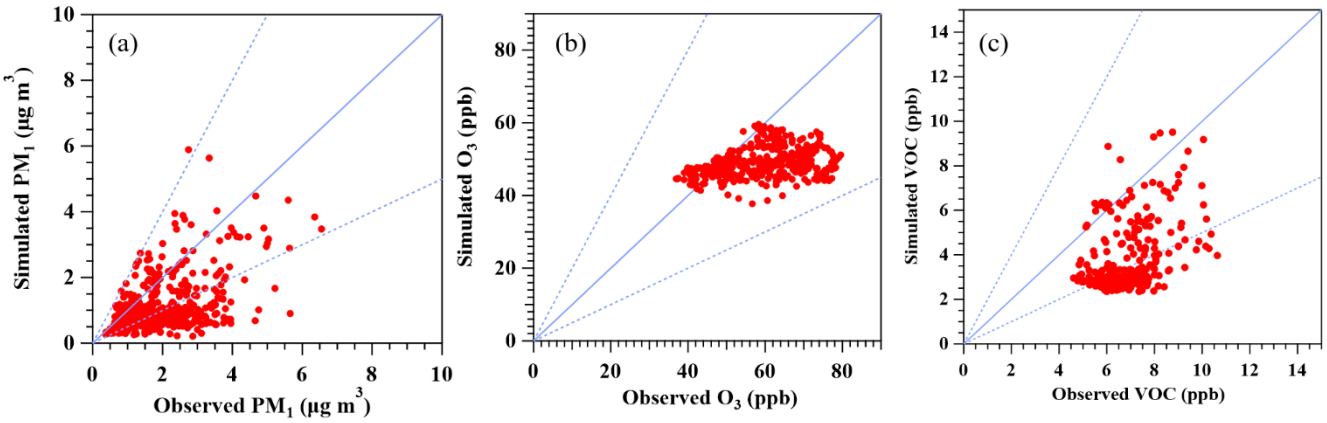

Figure S5. Comparison of simulated and observed PM (μg/m^3), O_3 (ppb) and VOC (ppb). PM, O_3 and VOC are hourly mean concentration.

Table S1. Model performance of meteorological factors at Nam Co station

	WS				RH				T			
	MB	**ME**	**RMSE**	**R**	**MB**	**ME**	**RMSE**	**R**	**MB**	**ME**	**RMSE**	**R**
Statistic	0.42	0.87	1.20	0.51	-1.38	12.20	16.30	0.67	0.07	1.85	2.43	0.89
Benchmarks	≤±0.5	≤2.0	≤2.0						≤±0.5	≤2.0		

MB: mean bias; ME: mean error; RMSE: root mean square error; R: correlation coefficient. The benchmarks were suggested by Boylan and Russell (2006).

Table S2. Model performance of the air pollutants at Nam Co station

	PM_1			O_3			VOC			SO_2		
	MFB	**MFE**	**R**	**NMB**	**NME**	**R**	**MFB**	**MFE**	**R**	**NMB**	**NME**	**R**
Statistic	0.49	0.50	0.72	0.14	0.23	0.51	-0.47	0.49	0.41			
Benchmarks	<±0.6	<0.75	>0.4	<±0.15	<0.35	>0.5						
References							<±0.77	<0.74		<±4.38	<±4.38	0.25-0.79

NMB: normalized mean bias; NME: normalized mean error; R: correlation coefficient; MFB: mean fractional bias; MFE: mean fractional error. The benchmarks for PM and O_3 were suggested by Emery et al. (2017) and Boylan and Russell (2006), respectively. The references for VOC and SO_2 were from Hu et al. (2017) and Mao et al. (2022), respectively.

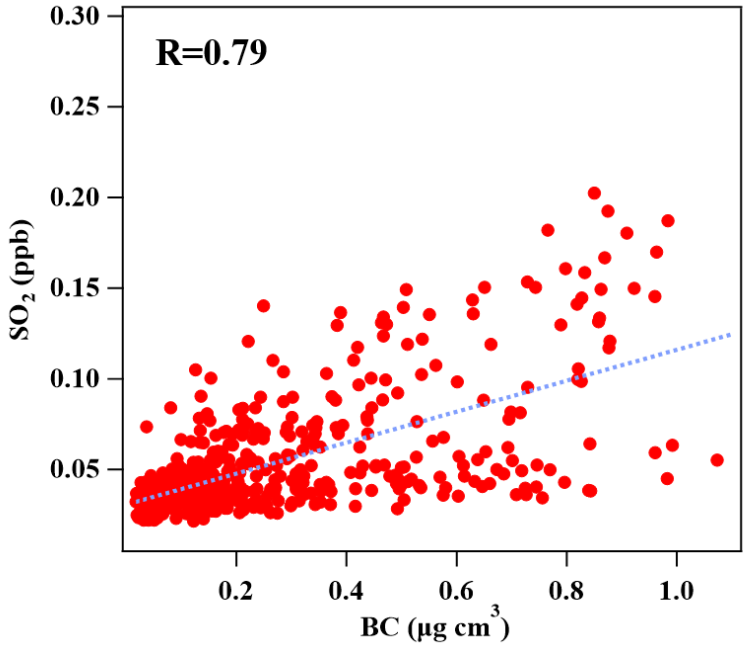

Figure S6. Relationship between SO_2 and BC at Mt. Yulong in 2015. The correlation coefficient R is 0.79.

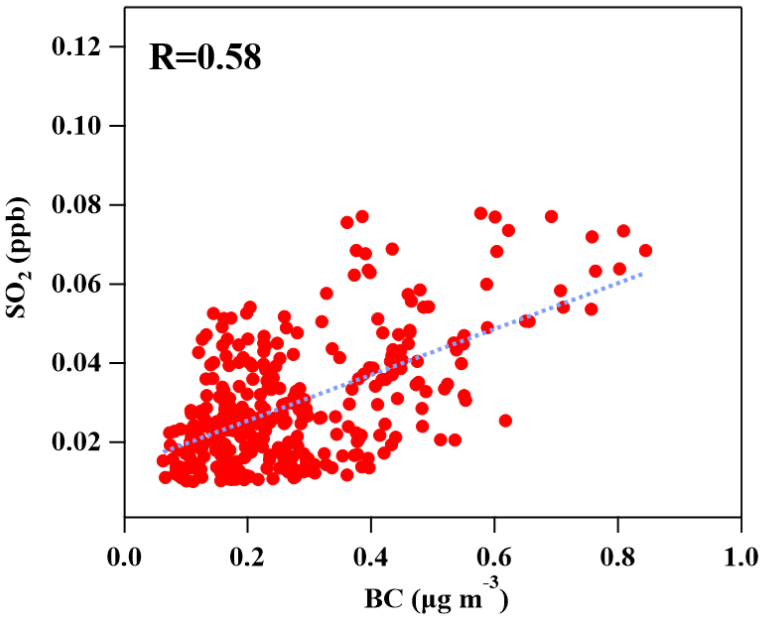

Figure S7. Relationship between modelled SO_2 and BC at Nam Co station. The correlation coefficient R is 0.58."

2. The observation period is a bit too short, especially, with only 10 days during monsoon. One cannot be sure that the high NPF frequency observed during this 10-day observation can be representative of the entire monsoon period.

Thanks for the comment. The measurements periods were a little short as the reviewer described, with about 4 weeks for the pre-monsoon season and 10 days for the monsoon season. But our measurements periods can be representative for this location during pre-monsoon season and monsoon season as follows: 1) The intensity of Indian Summer Monsoon during the two measurements periods can represent that in the whole pre-monsoon and monsoon seasons, respectively. The intensity of Indian Summer Monsoon is

an important indicator to distinguish the monsoon season. Here the intensity of Indian Summer Monsoon (ISM) was indicated by the ISM Index, which are defined by the negative outgoing longwave radiation anomalies (with respect to the climatological annual cycle) averaged over the Bay of Bengal–India region (10°–25°N, 70°–100°E) (Wang and Fan, 1999). As shown in Fig. R1, the measurement periods (green boxes) were in the pre-monsoon season (March-May) and monsoon season (June-September), respectively. And the IMS index during the two measurements periods were equivalent to those of the whole pre-monsoon season (average: -19.5 vs -20.7 W m^{-2}) and monsoon season (average: 27.0 vs 26.3 W m^{-2}), respectively. Therefore, we considered that these two observation periods are representative in the seasonal characteristics in pre-monsoon season and monsoon season, respectively.

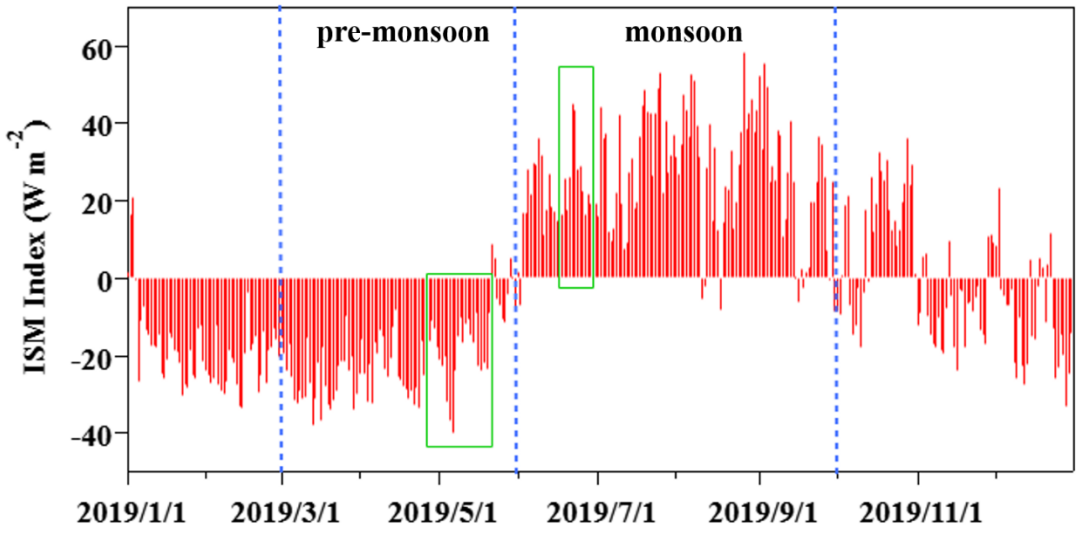

Figure R1. The Indian Summer Monsoon (ISM) Index in 2019. The measurements periods are marked by the green boxes.

2) The characteristics of meteorology and atmospheric pollutants in the two measurements periods was generally in agreement with the previous long-term studies at Nam Co station and other sites in the Tibetan Plateau (TP) (Yin et al., 2017; Cong et al., 2015; Bonasoni et al., 2010; Xu et al., 2018). Both previous research and this study showed that, strong westerlies pass through western Nepal, northwest India and Pakistan in pre-monsoon season, while air masses were mainly derived from Bangladesh and northeast India and brought moisture that originated in the Bay of Bengal in monsoon season (Fig. R2) (Yin et al., 2017). The temperature, WS and RH in the two measurements periods were matched with those in the whole pre-monsoon and monsoon season of 2020 at Nam Co station (Fig. R3) (National Tibetan Plateau Data Center). The average temperature in pre-monsoon and monsoon seasons were around 3 and 10 ℃, respectively. WS showed no difference between pre-monsoon and monsoon seasons with the average value of 4 m/s. The average level of RH was similar between the two seasons, but the variation range of

RH was larger in pre-monsoon season. In addition, the level of PM, BC and ozone in the two measurements periods were matched with those in the whole pre-monsoon and monsoon season at the other site of the TP (Fig. R4) (Bonasoni et al., 2010; Xu et al., 2018). The average concentrations of PM_1 ($PM_{0.8}$) in pre-monsoon and monsoon seasons were around 1 and 2 μg/m^3, respectively. The concentration of BC was at a level of hundreds nanogram per cubic meter in pre-monsoon season, while at a lower level in monsoon season. Ozone showed the similar pattern with BC. It should be noted that there will be some differences between this study and other results due to the differences in time resolution. In a word, the characteristics of meteorology and atmospheric pollutants in the two measurements periods in this study can well reflect those in pre-monsoon and monsoon seasons.

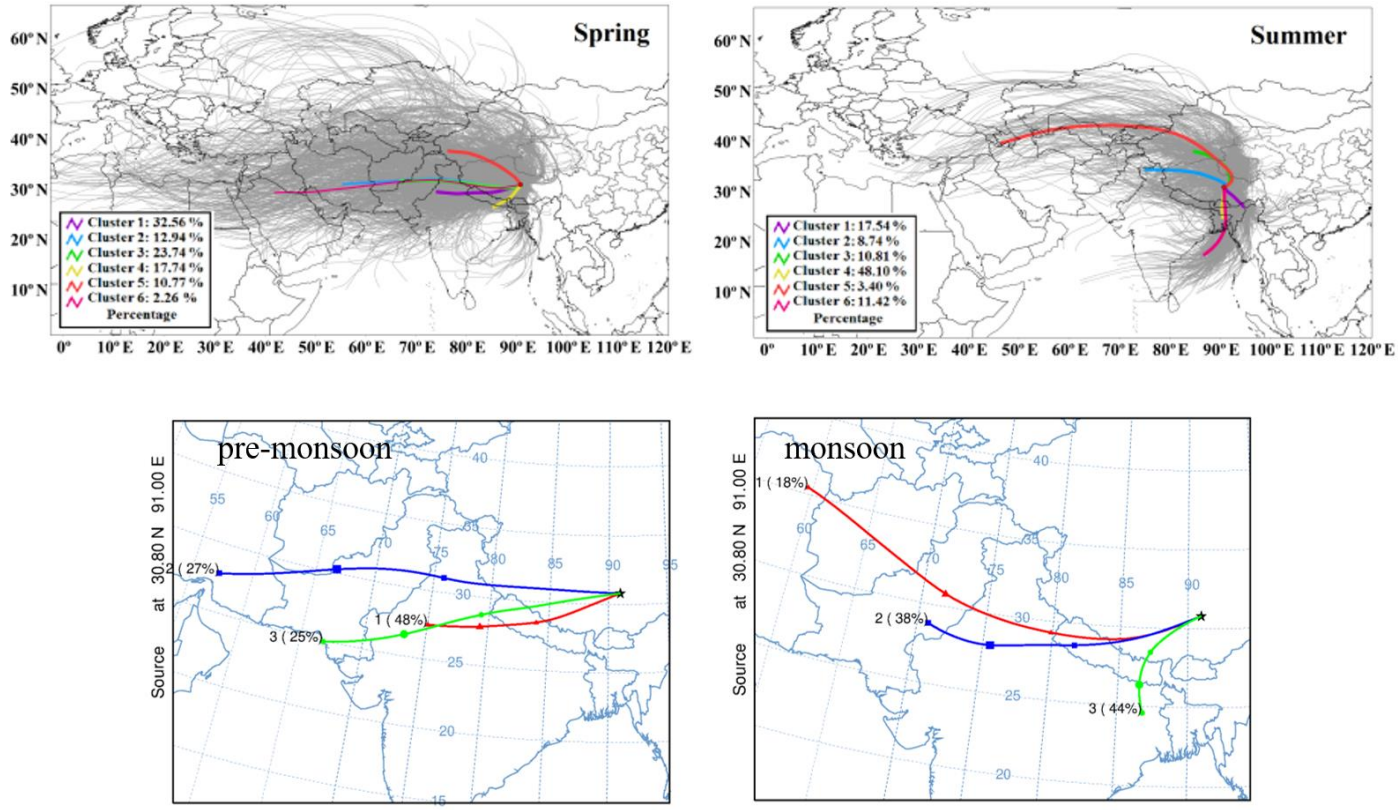

Figure R2. Comparison of trajectories between this study and previous study at Nam Co station. Backward HYSPLIT trajectories for each measurement day (black lines in the maps), and mean back trajectory for six HYSPLIT clusters (colored lines in the maps) arriving at Nam Co Station in spring (MAM) and summer (JJA) (Yin et al., 2017) (top). The frequencies of the 48 h back trajectories of air masses arriving at Nam Co station from different directions during pre-monsoon and monsoon seasons in this study (bottom).

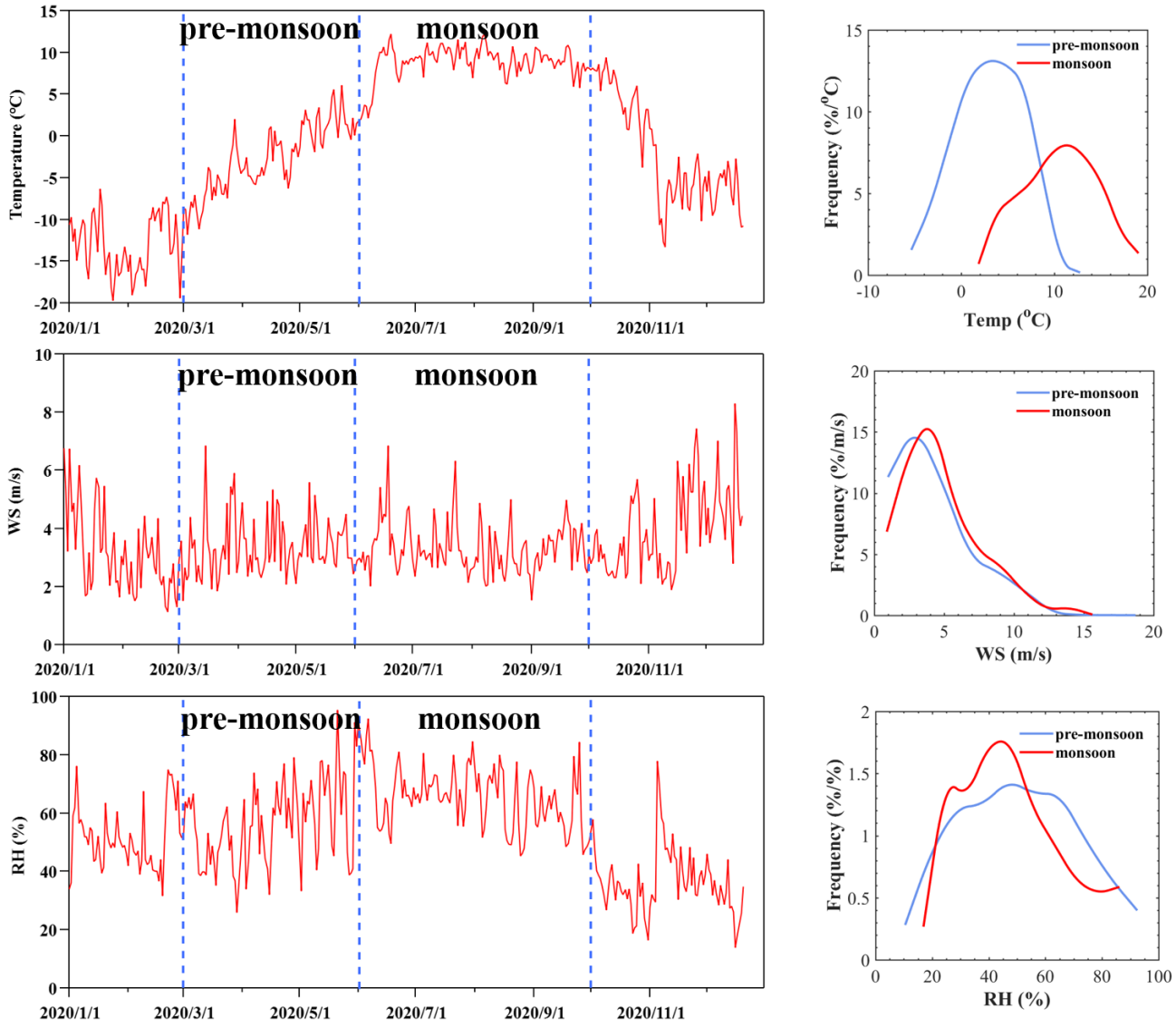

Figure R3. Comparison of meteorology between this study and the whole seasons in 2020. Time series of ambient temperature, wind speed and relative humidity at Nam Co station from January 2020 to December 2020 (National Tibetan Plateau Data Center) (left). Comparison in frequency distributions of temperature, WS and RH at Nam Co station in pre-monsoon and monsoon seasons in this study (right).

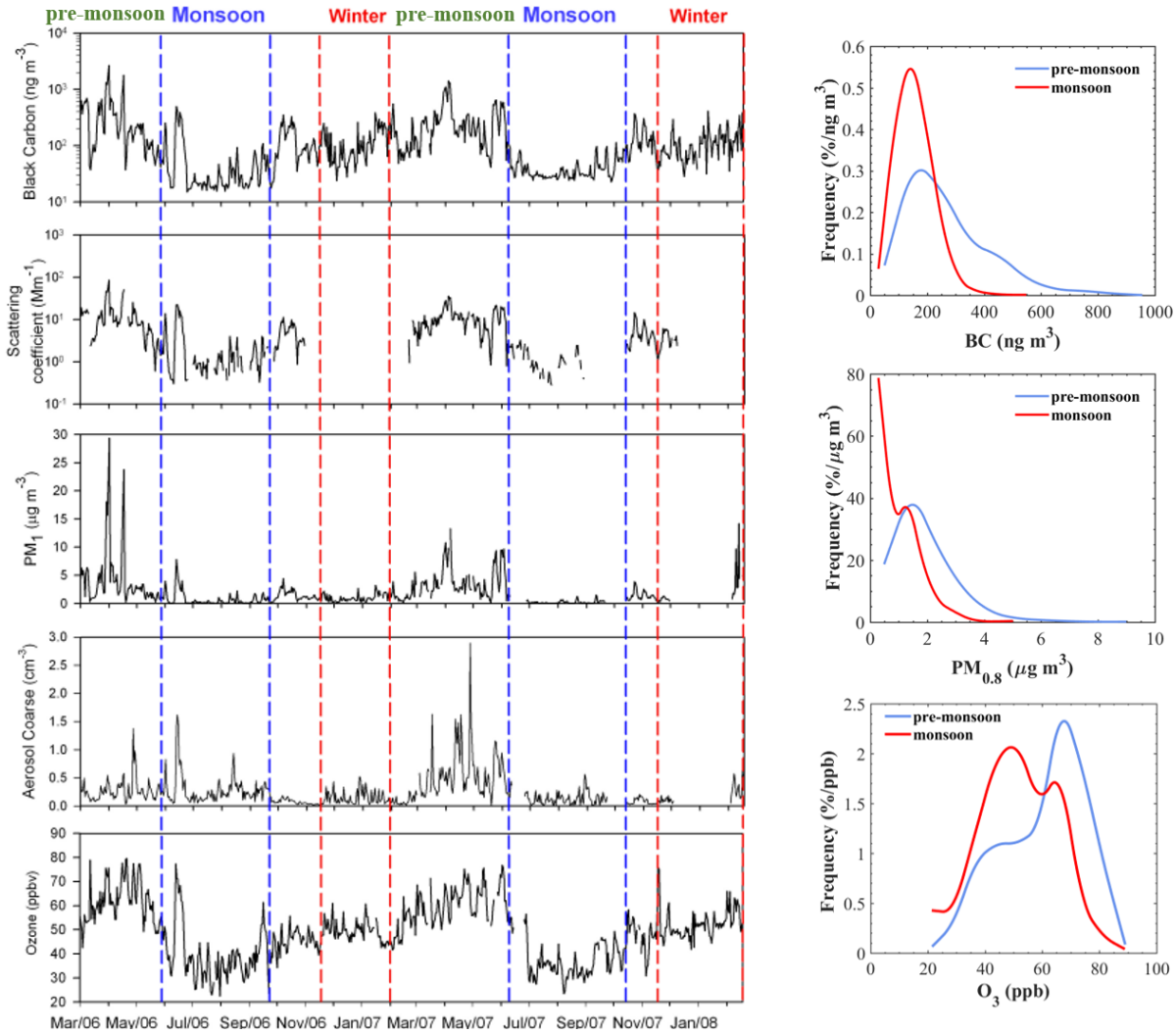

Figure R4. Comparison of atmospheric pollutants between this study and previous TP studies. Time series of f BC, aerosol scattering coefficient, PM_1, coarse particle number and surface ozone at the Nepal Climate Observatory-Pyramid (NCO-P) station from 1 March 2006 to 28 February 2008 (Bonasoni et al., 2010) (left). Comparison in frequency distributions of BC, $PM_{0.8}$ and O_3 at Nam Co station in pre-monsoon and monsoon seasons in this study (right).

3) Based on the above discussion, the two measurements periods in this study can respectively represent the pre-monsoon and monsoon season at Nam Co station, so the NPF characteristics of the two observation periods can also be considered as the NPF characteristics in pre-monsoon and monsoon seasons. It is true that we can not be sure that the extremely high NPF frequency observed during the 10-day observation period can be found in the entire monsoon season. But the difference of NPF frequency between the two seasons is very notable. Here we do not emphasize the absolute value of NPF frequency, but the significant difference of NPF frequency between two seasons. In addition, the phenomenon of higher NPF frequency in monsoon season than pre-monsoon season was also found in the other sites in the Tibetan Plateau (TP). A 16-month measurements from 2006 to 2007 at Himalayan Nepal Climate

Observatory at Pyramid (NCO-P) site on the southern TP showed NPF frequency of 38% in pre-monsoon season and 57% in monsoon season (Venzac et al., 2008). At Mt. Yulong on the southeastern TP, the NPF frequency was only 14% during pre-monsoon season (Shang et al., 2018). The NPF frequency of 15% in pre-monsoon season and 80% in monsoon season at Nam Co station was consistent with these studies, with more significant seasonal differences. The significant seasonal differences may be due to the fact that the occurrence of NPF is more sensitive to the monsoon in extremely clean background areas (such as Nam Co station and Mt. Yulong). In summary, our study emphasized the seasonal differences in NPF frequencies at Nam Co station, and the results was reliable.

Wang, B. and Fan, Z.: Choice of South Asian Summer Monsoon Indices, Bulletin of the American Meteorological Society, 80, 629-638, 10.1175/1520-0477(1999)080<0629:COSASM>2.0.CO;2, 1999.

Yin, X., Kang, S., de Foy, B., Cong, Z., Luo, J., Zhang, L., Ma, Y., Zhang, G., Rupakheti, D., and Zhang, Q.: Surface ozone at Nam Co in the inland Tibetan Plateau: variation, synthesis comparison and regional representativeness, Atmos. Chem. Phys., 17, 11293-11311, 10.5194/acp-17-11293-2017, 2017.

Cong, Z., Kang, S., Kawamura, K., Liu, B., Wan, X., Wang, Z., Gao, S., and Fu, P.: Carbonaceous aerosols on the south edge of the Tibetan Plateau: concentrations, seasonality and sources, Atmos. Chem. Phys., 15, 1573-1584, 10.5194/acp-15-1573-2015, 2015.

Bonasoni, P., Laj, P., Marinoni, A., Sprenger, M., Angelini, F., Arduini, J., Bonafè, U., Calzolari, F., Colombo, T., Decesari, S., Di Biagio, C., Di Sarra, A., Evangelisti, F., Duchi, R., Facchini, M. C., Fuzzi, S., Gobbi, G. P., Maione, M., Panday, A., Roccato, F., Sellegri, K., Venzac, H., Verza, G., Villani, P., Vuillermoz, E., and Cristofanelli, P.: Atmospheric Brown Clouds in the Himalayas: first two years of continuous observations at the Nepal Climate Observatory-Pyramid (5079 m), Atmospheric Chemistry and Physics, 10, 7515-7531, 10.5194/acp-10-7515-2010, 2010.

Xu, J., Zhang, Q., Shi, J., Ge, X., Xie, C., Wang, J., Kang, S., Zhang, R., and Wang, Y.: Chemical characteristics of submicron particles at the central Tibetan Plateau: insights from aerosol mass spectrometry, Atmos. Chem. Phys., 18, 427-443, 10.5194/acp-18-427-2018, 2018.

Junbo, W.: Daily meteorological Data of Nam Co Station China during 2019-2020, National Tibetan Plateau Data Center [dataset], 10.11888/Meteoro.tpdc.271782, 2021.

Venzac, H., Sellegri, K., Laj, P., Villani, P., Bonasoni, P., Marinoni, A., Cristofanelli, P., Calzolari, F., Fuzzi, S., Decesari, S., Facchini, M.-C., Vuillermoz, E., and Verza, G. P.: High frequency new particle formation in the Himalayas, Proceedings of the National Academy of Sciences, 105, 15666-15671, doi:10.1073/pnas.0801355105, 2008.

Shang, D., Hu, M., Zheng, J., Qin, Y., Du, Z., Li, M., Fang, J., Peng, J., Wu, Y., Lu, S., and Guo, S.: Particle number size distribution and new particle formation under the influence of biomass burning at a high altitude background site at Mt. Yulong (3410 m), China, Atmos. Chem. Phys., 18, 15687-15703, 10.5194/acp-18-15687-2018, 2018.

Due to harsh conditions and logistical limitations, our observation periods were limited. However, our conclusions are obvious and representative, and we will carry out more detailed observations for a longer period in the future if possible. To illustrate the representativeness of the observation periods, we have made supplements in the revised manuscript as follows:

"**2.1 Measurement site**

The measurement was conducted from 26 April to 22 May, 2019 and 15 June to 25 June, 2019, and can be representative of the pre-monsoon season and the summer monsoon season, respectively (Text S1) (Bonasoni et al., 2010; Cong et al., 2015)."

"**Text S1 The representativeness of the observation periods**

The measurement was conducted from 26 April to 22 May, 2019 and 15 June to 25 June, 2019, and can be representative of the pre-monsoon season and monsoon season, respectively.

Firstly, the intensity of Indian Summer Monsoon during the two measurements periods can represent that in the whole pre-monsoon and monsoon seasons, respectively. The intensity of Indian Summer Monsoon is an important indicator to distinguish the monsoon season. Here the intensity of Indian Summer Monsoon (ISM) was indicated by the ISM Index, which are defined by the negative outgoing longwave radiation anomalies (with respect to the climatological annual cycle) averaged over the Bay of Bengal–India region (10°–25°N, 70°–100°E) (Wang and Fan, 1999). As shown in Fig. S1, the measurement periods (green boxes) were in the pre-monsoon season (March-May) and monsoon season (June-September), respectively. And the IMS index during the two measurements periods were equivalent to those of the whole pre-monsoon season (average: -19.5 vs -20.7 W m-2) and monsoon season (average: 27.0 vs 26.3 W m-2), respectively.

Secondary, the characteristics of meteorology and atmospheric pollutants in the two measurements periods was generally in agreement with the previous long-term studies at Nam Co station and other sites in the Tibetan Plateau (TP) (Yin et al., 2017; Cong et al., 2015; Bonasoni et al., 2010; Xu et al., 2018). That is, the characteristics of meteorology (temperature, WS and RH) and atmospheric pollutants (PM, BC and ozone) in the two measurements periods were matched with those in the whole pre-monsoon and monsoon season at Nam Co station and other sites in the TP.

Therefore, the two observation periods are representative in the seasonal characteristics in pre-monsoon season and monsoon season, respectively.

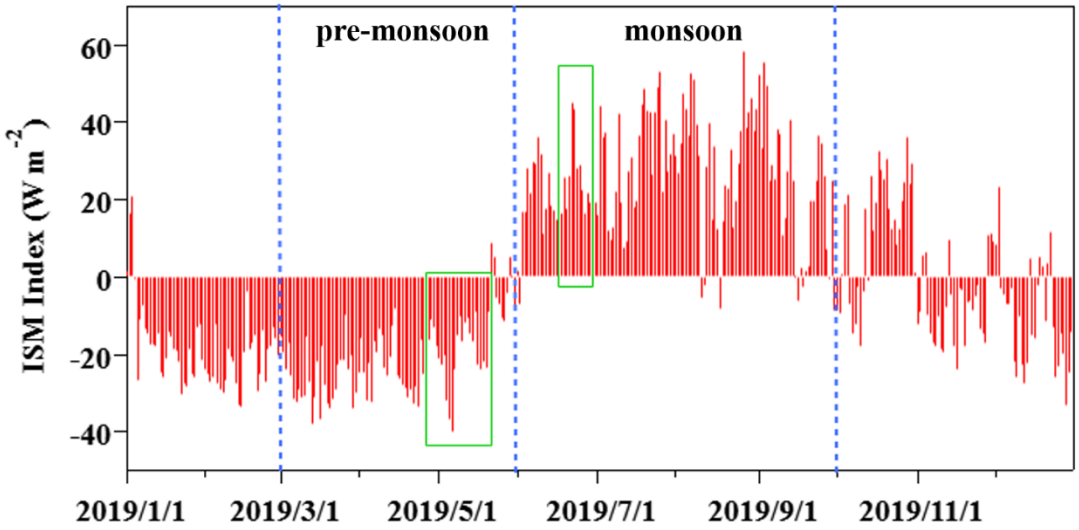

Figure S1. The Indian Summer Monsoon (ISM) Index in 2019. The measurements periods are marked by the green boxes."

3. The authors grouped their data into "NPF-pre days", "NPF-monsoon days" and "non-event days" in

Fig. 3- Fig. 7 and related discussions. I may suggest separating "non-event days" into pre-monsoon and monsoon non-event days.

Thanks for the comment. There were no typical "non-event days" in monsoon season according to the classification of NPF events. The two days which were not "NPF days" in monsoon season were "undefined days", as in which the increase of PN_{3-10} was observed without the particles growing to the larger size (24 June, 2019), or we can see the later phase of a mode growing in the Aitken mode size range (18 June, 2019) (Dal Maso et al., 2005). The particle number size distributions in 18 June and 24 June, 2019 are present in Fig. R5b and c, and a typical NPF event in 23 June, 2019 is shown in Fig. R5a.

Dal Maso, M., Kulmala, M., Riipinen, I., and Wagner, R.: Formation and growth of fresh atmospheric aerosols: Eight years of aerosol size distribution data from SMEAR II, Hyytiälä, Finland, Boreal Environment Research, 10, 323-336, 2005.

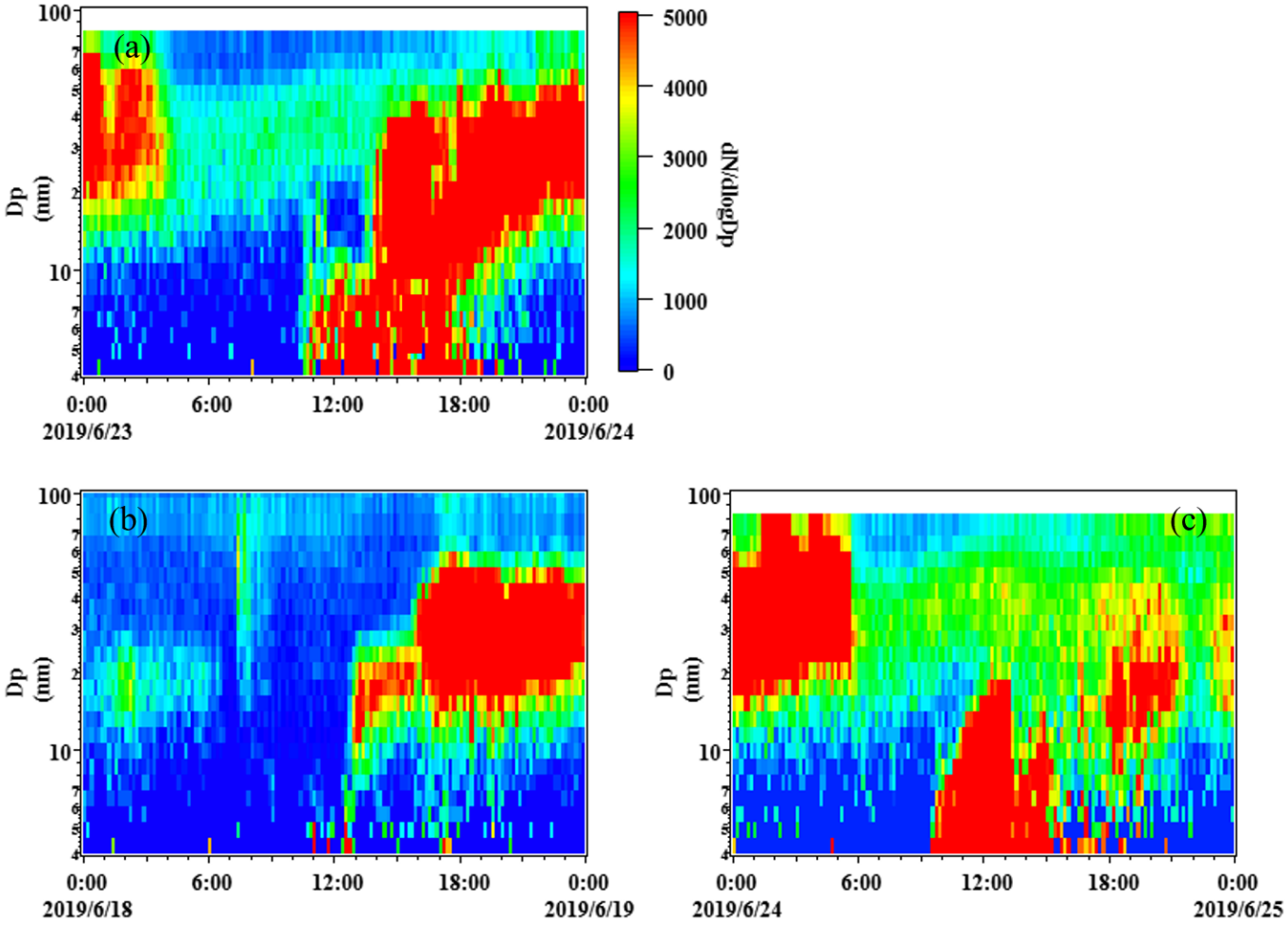

Figure R5. The particle number size distribution in (a) 23 June, 2019 (NPF day), (b) 18 June, 2019 (undefined day), and (c) 24 June, 2019 (undefined day).

At the same time, we also analyzed the atmospheric characteristics in "undefined days" in monsoon season (Fig. R6). And we found that the atmospheric characteristics including CS, $J(O^1D)$, temperature, RH, wind speed, water content in "undefined days" in monsoon season were comparable with those in

"NPF days" in monsoon season. Considering that the purpose is to find the difference between "NPF days" and "non-event days", we did not add the two "undefined days" in the manuscript.

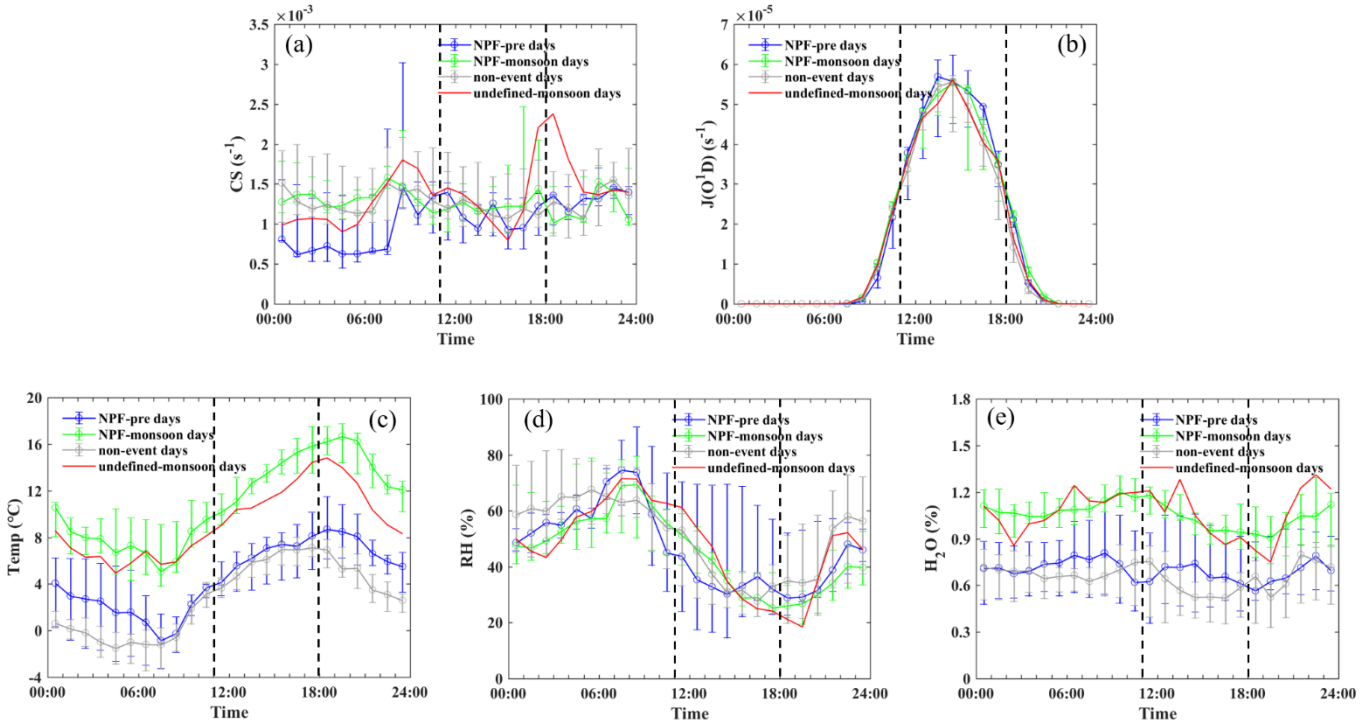

Figure R6. The Diurnal variations of (a) condensation sink (CS), (b) JO^1D, (c) temperature, (d) RH, and (e) H_2O in NPF-pre days, NPF-monsoon days, non-event days and undefined days in monsoon season (undefined-monsoon days).